doi:10.1246/cl.2011.699
Published on the web June 4, 2011

Design, Synthesis, and Characterization of Self-assembled Peptide Nanostructures toward Peptide-directed Biomineralization

Kin-ya Tomizaki,*[1,2] Tatsuki Kotera,[2] Hideki Naito,[2] Shota Wakizaka,[2] and Shin-ichi Yamamoto[3]
[1]*Innovative Materials and Processing Research Center, Ryukoku University, Seta, Otsu, Shiga 520-2194*
[2]*Department of Materials Chemistry, Ryukoku University, Seta, Otsu, Shiga 520-2194*
[3]*Department of Electronics and Informatics, Ryukoku University, Seta, Otsu, Shiga 520-2194*

(Received April 12, 2011; CL-110310; E-mail: tomizaki@rins.ryukoku.ac.jp)

There is increasing interest in nanostructures and in the molecular design of building blocks which self-assemble into nanoscaled intelligent materials. We outline a method for controlling the nanostructures of amphiphilic nonapeptides by changing the pH of the aqueous medium. A lysine residue on the hydrophilic face of the peptide plays a critical role as a morphology-control unit. This self-assembling peptide may, therefore, find application as a template for peptide-directed biomineralization.

Biology provides the major source of inspiration for the design of organic–inorganic hybrid materials (biominerals), pursued in our laboratory using a bottom-up approach. In the formation of biominerals, proteins play an important role to control their morphologies as seen in bone, dentin, mollusk shells, skeletons, and larval spicules.[1] However, the manipulation of proteins on a large scale is quite costly and laborious. In the context of industrialization, we are now focusing on the use of synthetic peptides as a template to fabricate well-organized biominerals. One of the key elements for peptide-directed biomineralization is to increase the diversity in the morphologies of template nanostructures. The amphiphilicity of peptides is attractive for incorporation into fabricated, tailored nanostructures.[2] The self-assembly of amphiphilic molecules is driven by weak noncovalent interactions such as hydrogen bonding, van der Waals forces, electrostatic interactions, hydrophobic interactions, and π–π stacking effects. The cumulative effect of these weak interactions is sufficient to organize nanometer- to micrometer-sized supramolecular structures. Thus, the self-assembly of β-sheet-forming amphiphilic peptides is a powerful strategy for developing intelligent materials, and much effort has been devoted to this endeavor.[3–11]

Recently, Shao and Parquette reported that peptide–dendron hybrids (PDH) interconvert between fibrous and nanotube aggregates upon change in the pH of the medium.[12] The attenuation of electrostatic repulsions between intermolecular lysine residues (Lys) was a key factor controlling these changes in aggregation state. Clearly, the ability to increase the diversity in morphologies of template nanostructures through simple physical manipulations would be a promising approach to the development of bio-nanoprocesses leading to intelligent materials.[13] Herein, we show the critical role played by a Lys residue at the hydrophilic face of an amphiphilic nonapeptide in controlling the morphology (plate-like, flattened assembly or fibrous assembly) of peptide-based nanostructures to diversify the template morphologies toward peptide-directed biomineralization. The results of a Nile Red encapsulation assay provide insights into the interior of these peptide nanostructures.

(A)

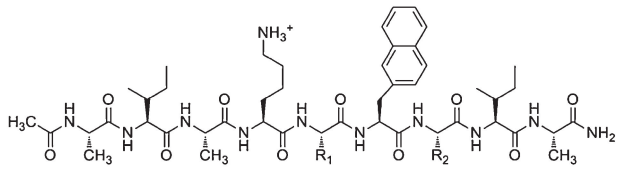

Peptide	R_1	R_2
RU-001	-$(CH_2)_2COO^-$ (Glu)	-$(CH_2)_4NH_3^+$ (Lys)
RU-002	-$(CH_2)_2COO^-$ (Glu)	-CH_3 (Ala)

(B)

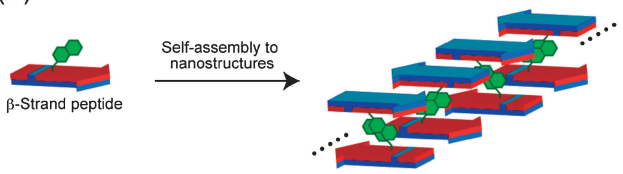

Figure 1. (A) Molecular design of amphiphilic nonapeptides **RU-001** and **RU-002** used in this study. (B) Self-assembly of peptides to form flattened or fibrous structures. Hydrophobic amino acid residues are shown in red, hydrophilic ones in blue, and 2-naphthylalanine [Nal(2)] in green.

Amphiphilic nonapeptides **RU-001** and **RU-002** were designed to have two isoleucines (Ile) and a 2-naphthylalanine [Nal(2)] at one face, which provides the driving force for self-assembly via hydrophobic interaction (Figure 1). Alanines (Ala) and a glutamic acid (Glu) were placed at another face to make the peptides water-soluble. A Lys residue at the hydrophobic face was expected to stabilize the peptide assembly through inter- and/or intramolecular cation–π interactions between its ammonium moiety and the naphthyl side chain. This Lys would also aid solubilization of intermediates during self-assembly. Another Lys residue was placed at the hydrophilic face in **RU-001** to act as a pH-responsive unit. For the reference peptide, this Lys residue in **RU-001** was replaced with an Ala in **RU-002**.

Both peptides were prepared by standard solid-phase peptide synthesis using Fmoc chemistry,[14] purified by reverse-phase HPLC, and characterized by MALDI-TOF-MS. Peptide stock solutions were prepared by dissolving the purified peptide in 2,2,2-trifluoroethanol (TFE) to prevent self-assembly during storage. The concentration of each stock solution was determined by UV–vis spectroscopy using an extinction coefficient of 5500 $M^{-1}\,cm^{-1}$ for the Nal(2) residue in aqueous solution containing 1% TFE (v/v).[15] The peptide stock solution in TFE was transferred into a microtube, dried with a N_2 gas stream, then dried in vacuo for 30 min. Solvent was added to the

microtube, and the obtained aqueous solution was sonicated at 50 °C for 2 min, incubated at 40 °C for 1 day, and then at 25 °C for more than 7 days. For peptide-directed $CaCO_3$ mineralization, ultrapure water (water) is necessary to avoid metal contamination, and peptide-directed silicification requires high pH to accelerate hydrolysis of tetraalcohoxysilane and maintain pH against generating silicic acid. Thus, we employed two different solvent systems, water and 0.1 M Tris-HCl (pH 10) to characterize peptide nanostructures as templates toward peptide-directed biomineralization.

The conformational properties of **RU-001** and **RU-002** were first investigated by measuring the ATR-FTIR spectra of peptide films prepared from aqueous solutions of **RU-001** or **RU-002** matured in water (Figure 2). The amide I region, originating from the amide carbonyl stretching frequencies between 1600 and 1700 cm^{-1}, is often used to assess the amide mode. ATR-FTIR spectra of **RU-001** and **RU-002** revealed that both peptides exhibit a strong amide I band around 1625 cm^{-1} and a weak band around 1675 cm^{-1}, indicating that the self-assembled nanostructures are composed predominantly of antiparallel β-sheet conformation.[16,17] ATR-FTIR spectra of **RU-001** and **RU-002** in 0.1 M Tris-HCl (pH 10) could not be obtained due to salt precipitation.

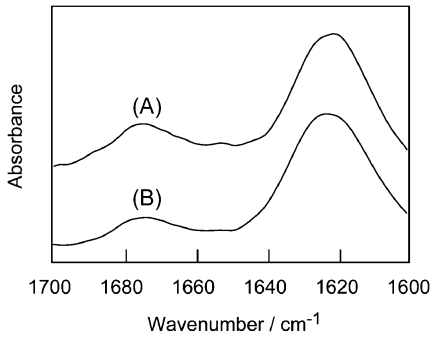

Figure 2. ATR-FTIR spectra of peptide films prepared from aqueous solutions of **RU-001** (A) and **RU-002** (B) matured for more than 7 days ([peptide] = 1.0 mM in water, pH ≈6).

The nanostructures of the peptide assemblies on Si(100) surfaces were characterized by atomic force microscopy (AFM). Figure 3 shows the tapping-mode AFM images of **RU-001** and **RU-002** matured in aqueous solution for more than 7 days. AFM images of **RU-001** matured in water revealed the presence of plate-like, flattened assemblies ca. 100 nm in width and ca. 1 nm in height (Figure 3A). Surprisingly, AFM images of **RU-001** matured in 0.1 M Tris-HCl (pH 10) showed nanofibers ca. 2 μm in length and ca. 10 nm in height (Figure 3B). In water, the Lys side chain at the hydrophilic face of **RU-001** was expected to bear an ammonium cation, which would cause electrostatic repulsion between the peptides, thereby destabilizing nanofiber formation. By increasing the pH to 10, which is close to the pK_a of the Lys side chain, peptide nanofiber formation by **RU-001** was stabilized due to the attenuation of electrostatic repulsions.

All AFM images of **RU-002** matured in three different solvent systems, water, 0.1 M Tris-HCl (pH 7.4), and 0.1 M Tris-HCl (pH 10) showed micrometer-long fibers. This suggest that self-assembly of **RU-002** was predominantly affected by pH of the solvent systems and that salt effects are relatively limited, representatively shown are fibers with ca. 2 μm length and ca. 10 nm height matured in water and pH 10 in Figures 3C and 3D, respectively. However, it seemed that increasing pH to 10 somewhat reduced the number of the nanofibers of **RU-002** relative to that in water (also pH 7.4, data not shown). Differences in morphological features of these two peptides would likely stem from the Lys residue at the hydrophilic face acting as a pH-sensitive morphology-control unit.

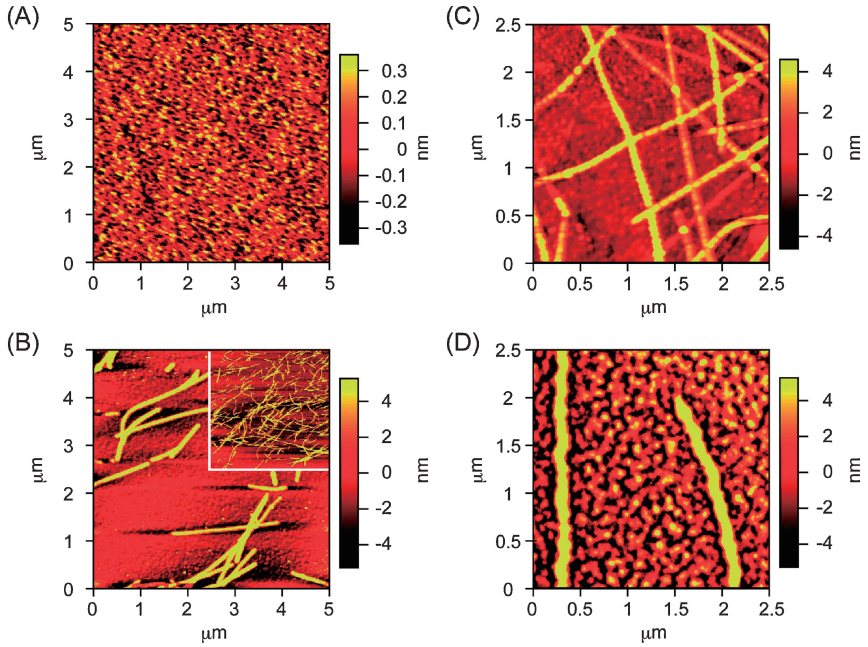

Figure 3. Tapping-mode AFM images of **RU-001** (A and B) and **RU-002** (C and D) matured in water (pH ≈ 6) (A and C) and 0.1 M Tris-HCl (pH 10) (B and D) matured for more than 7 days. Inset: tapping-mode AFM image of the expanded area of B, 20 μm × 20 μm.

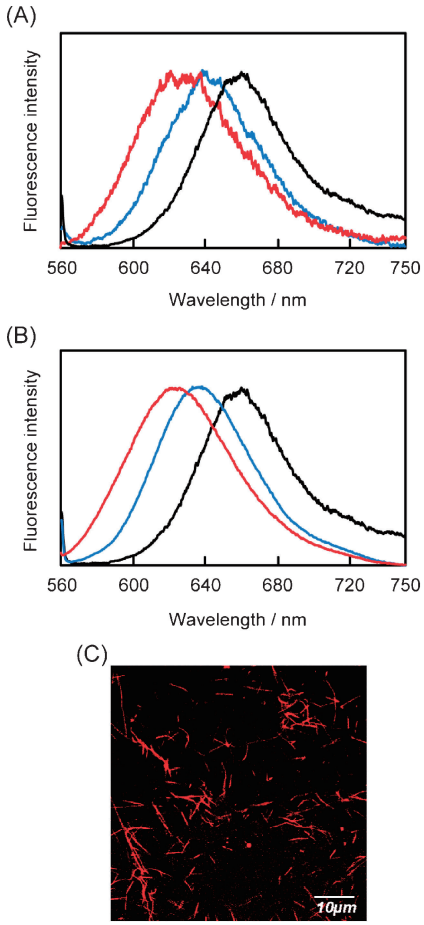

Figure 4. Fluorescence spectra ($\lambda_{ex} = 550$ nm) of Nile Red encapsulated by **RU-001** (A) and **RU-002** (B) in water (pH ≈ 6) (blue lines) and 0.1 M Tris-HCl (pH 10) (red lines) matured for more than 7 days. Fluorescence spectra ($\lambda_{ex} = 550$ nm) of Nile Red alone in water are shown as black lines (A and B). All fluorescence spectra were normalized for clarity. (C) Confocal laser scanning micrograph of the nanostructures of **RU-002** encapsulating Nile Red in water ($\lambda_{ex} = 543$ nm and $\lambda_{em} = 555$–655 nm). [Nile Red] = 2 μM and [peptide] = 100 μM.

Meanwhile, the peptide assemblies sequester hydrophobic amino acid side chains from the aqueous phase into the nanostructure interior. These interiors were assessed using a Nile Red encapsulation assay. Nile Red is a neutral, polarity-sensitive, and water-insoluble dye. It enters the hydrophobic interior of peptide nanostructures as they mature; this sequestering from water causes a significant blue shift in the fluorescence spectrum.[12] Figure 4 shows the results of the Nile Red encapsulation assay with **RU-001** matured in water or 0.1 M Tris-HCl (pH 10). Nile Red exhibited fluorescence emission at 640 nm in the presence of **RU-001** in water, which was clearly blue-shifted relative to its emission in the absence of the peptide (660 nm) (Figure 4A). Nile Red encapsulated by **RU-001** in 0.1 M Tris-HCl (pH 10) also yielded a blue-shifted fluorescence spectrum (620 nm) compared with dye alone in water (660 nm) (Figure 4A). Likewise, we also conducted Nile Red encapsulation assays with **RU-002** matured in water and 0.1 M Tris-HCl (pH 10). The fluorescence spectrum of Nile Red encapsulated by **RU-002** either in water or in 0.1 M Tris-HCl (pH 10) was blue-shifted (640 and 620 nm, respectively) compared with the dye alone in water (660 nm) (Figure 4B). These results suggest that Nile Red dye was encapsulated by the hydrophobic interiors of the peptide nanostructures. As described in the literature,[12] Nile Red encapsulated by a peptide–dendron hybrid (PDH) in water exhibited fluorescence emission at 618 nm. This value is comparable to that of **RU-001** and **RU-002** in 0.1 M Tris-HCl (pH 10) (620 nm) but is somewhat blue-shifted from that obtained for Nile Red encapsulated by **RU-001** and **RU-002** in water (640 nm), probably due to the cationic Lys side chain at the hydrophobic face increasing the polarity of the nanostructure interior. We also directly observed the nanostructures of **RU-002** encapsulating Nile Red in water using a confocal laser scanning microscope (Figure 4C). A number of nanofibers ca. 5 μm in length were highlighted more brightly than the water phase. These results suggest that hydrophobic packing assisted β-sheet assembly. Hydrophobic packing also helped maintain the well-organized structures into fibers and flattened assembly (Figure 1B).

We have demonstrated a method for controlling the nanostructures of amphiphilic nonapeptides by changing the pH of the aqueous medium. The Lys residue at the hydrophilic face of the **RU-001** plays a critical role as a morphology-control unit. The interior of the peptide nanostructures is hydrophobic, allowing encapsulation of hydrophobic molecules. The described peptide-directed nano-bioprocess would be a promising approach for the development of biocompatible, intelligent organic–inorganic hybrid materials by increasing in the diversity of template morphologies (e.g., fibrous, spherical, and flattened assemblies). However, how the peptide building blocks align in the well-organized nanostructures described above (e.g., existence of cation–π interactions and the role of Lys residue at the hydrophobic face) remains unclear, which is currently being investigated by measuring 2D NMR.

This study was supported in part by the Ryukoku University Science and Technology Fund. We would like to thank Professor Hisakazu Mihara (Tokyo Institute of Technology, Japan) for assistance with ATR-FTIR measurements. We are also grateful to Professor Itaru Hamachi (Kyoto University, Japan) for assistance with confocal laser scanning microscope imaging.

References

1 A. Sugawara, T. Nishimura, Y. Yamamoto, H. Inoue, H. Nagasawa, T. Kato, *Angew. Chem., Int. Ed.* **2006**, *45*, 2876.
2 T. Shimizu, M. Masuda, H. Minamikawa, *Chem. Rev.* **2005**, *105*, 1401.
3 I. W. Hamley, *Angew. Chem., Int. Ed.* **2007**, *46*, 8128.
4 R. V. Ulijn, A. M. Smith, *Chem. Soc. Rev.* **2008**, *37*, 664.
5 H. Cui, M. Webber, S. I. Stupp, *Biopolymers* **2010**, *94*, 1.
6 S. Cavalli, F. Albericio, A. Kros, *Chem. Soc. Rev.* **2010**, *39*, 241.
7 R. J. Brea, C. Reiriz, J. R. Granja, *Chem. Soc. Rev.* **2010**, *39*, 1448.
8 D. M. Marini, W. Hwang, D. A. Lauffenburger, S. Zhang, R. D. Kamm, *Nano Lett.* **2002**, *2*, 295.
9 S. Matsumura, S. Uemura, H. Mihara, *Chem.—Eur. J.* **2004**, *10*, 2789.
10 S. E. Paramonov, H.-W. Jun, J. D. Hartgerink, *J. Am. Chem. Soc.* **2006**, *128*, 7291.
11 H. Xu, J. Wang, S. Han, J. Wang, D. Yu, H. Zhang, D. Xia, X. Zhao, T. A. Waigh, J. R. Lu, *Langmuir* **2009**, *25*, 4115.
12 H. Shao, J. R. Parquette, *Angew. Chem., Int. Ed.* **2009**, *48*, 2525.
13 M. B. Dickerson, K. H. Sandhage, R. R. Naik, *Chem. Rev.* **2008**, *108*, 4935.
14 W. C. Chan, P. D. White, *Fmoc Solid Phase Peptide Synthesis: A Practical Approach*, ed. by W. C. Chan, P. D. White, Oxford University Press, New York, **2000**, pp. 41–76.
15 M. Sadqi, L. J. Lapidus, V. Muñoz, *Proc. Natl. Acad. Sci. U.S.A.* **2003**, *100*, 12117.
16 A. Dong, P. Huang, W. S. Caughey, *Biochemistry* **1990**, *29*, 3303.
17 S. Srisailam, H.-M. Wang, T. K. S. Kumar, D. Rajalingam, V. Sivaraja, H.-S. Sheu, Y.-C. Chang, C. Yu, *J. Biol. Chem.* **2002**, *277*, 19027.

